Reflectance and resistivity of barely metallic $LaTiO_3$

D. A. Crandles and T. Timusk
Department of Physics, McMaster University, Hamilton, Ontario, Canada L8S 4M1

J. E. Greedan
Institute for Materials Research and Department of Chemistry, McMaster University, Hamilton, Ontario, Canada L8S 4M1

(Received 20 June 1991)

The absolute reflectance of $LaTiO_3$ was measured from 70 to 17 500 cm^{-1}. The Kramers-Kronig-derived optical conductivity shows three sharp phonon structures near 170, 340, and 540 cm^{-1} that are explained by a factor-group analysis. The midinfrared spectrum is dominated by a broad absorption band with an onset near 600 cm^{-1}. A comparison of reflectance and resistivity measurements indicates that the dc mobility is less than 3 cm^2/V s at 300 K, and thus the carriers are somewhat localized.

I. INTRODUCTION

$LaTiO_3$ is a member of the isostructural series of compounds $RTiO_3$ where R is a rare-earth element. The electrons associated with the Ti^{3+} ion in these compounds can be either localized as in $GdTiO_3$ or apparently itinerant as in $LaTiO_3$.[1]

Early work[2-5] suggested that $LaTiO_3$ undergoes a metal-insulator transition near 130 K. Above the transition temperature the resistivity increases with temperature in a metallic fashion and $LaTiO_3$ shows a temperature-independent magnetic susceptibility. Below the transition temperature the resistivity is semiconductorlike, and $LaTiO_3$ orders antiferromagnetically. Recent experiments on the $LaTiO_x$ system have indicated that the electrical and magnetic properties are highly sensitive to oxygen stoichiometry.[6,7]

$LaTiO_3$ has a nonempty $3d$ band, and recent band-structure calculations, assuming a cubic perovskite structure, predict metallic behavior.[8] However, as the dc conductivity of $LaTiO_3$ is below the Mott minimum[9] ($\approx 150\ \Omega^{-1}cm^{-1}$) at all temperatures, the nature of the conduction mechanism is unclear. Oxides have long been studied for their wide range in dc conductivities, often inexplicable in terms of one-electron band models.[10-12] Optical measurements have provided much insight into the transport and electronic properties of these curious materials. For example, absorption measurements established polaronic conduction TiO_2,[13,14] while reflectivity measurements established[15,16] the magnitude of the gap which opened up at the Fermi surface during the metal-insulator transition in VO_2. More recently, the evolution of the optical conductivity in the copper oxides, from the undoped antiferromagnetic insulating phase to the moderately doped superconducting phase, has been established.[17,18]

In this paper, reflectance measurements are presented for a well-characterized sample of $LaTiO_3$ and various explanations for the optical and transport properties are considered.

II. SAMPLE CHARACTERIZATION

Single crystals were prepared by melting $LaTiO_3$ in an open molybdenum crucible under argon using rf heating. The sample studied had stoichiometry $La_{0.98\pm0.04}TiO_{3.03\pm0.05}$ as determined by neutron activation and thermogravimetric analyses. The lattice constants of the sample were 5.6204(6), 5.6035(7), and 7.911(1) Å determined using a Guinier camera, and are in reasonable agreement with previous neutron-diffraction data.[19] The reflectance, magnetization, and resistivity measurements to be reported below were all made on the same crystal.

Magnetization measurements performed on a SQUID magnetometer are shown in Fig. 1. The sample was cooled to 5 K in zero field. The field was then increased to 10 kG where the magnetization was almost saturated. Finally, the field was reduced to zero and the moment measured as the sample warmed. The same behavior is

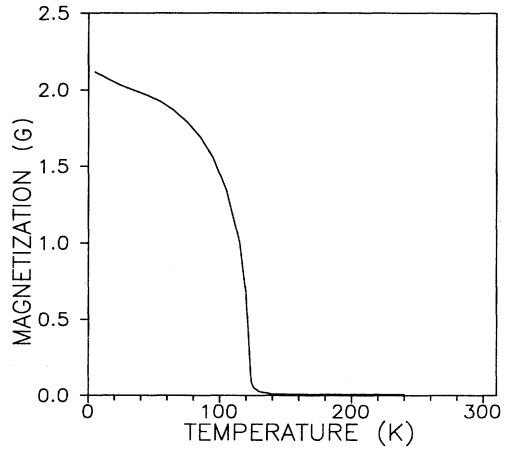

FIG. 1. Magnetization of $LaTiO_3$ vs temperature obtained on a SQUID magnetometer. The sample was cooled in zero field, the saturation magnetization established in a 10-kG field, and finally the magnetization measured by warming in zero field.

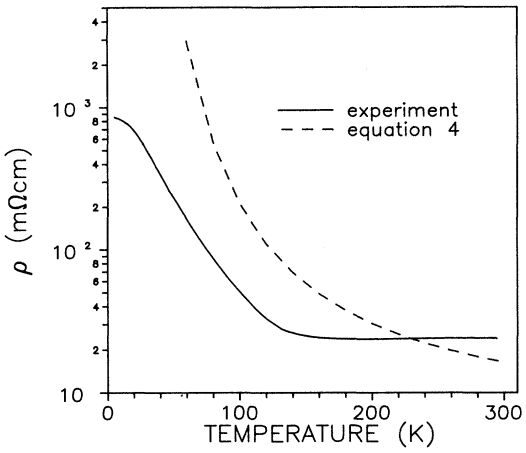

FIG. 2. Comparison of measured resistivity vs temperature with the predictions of narrow-band-semiconductor model [Eq. (4)].

observed as reported previously where the small ferromagnetic moment seen in Fig. 1 is due to canting of adjacent spins.[1,2,5]

Resistivity measurements, made with silver paint contacts in the Van de Pauw configuration, showed the change from metallic to insulating behavior near 175 K as seen in Fig. 2.

III. RESULTS

The reflectance of $LaTiO_3$ was obtained at 300 K using Fourier-transform spectroscopy for frequencies between 70 and 5500 cm^{-1} on a mechanically polished crystal. The reflectance at higher frequencies (up to 17 500 cm^{-1}) was measured by grating spectroscopy. To measure the absolute reflectance correctly, the effect of surface roughness must be eliminated. After measuring the reflectance of the sample versus a stainless-steel reference, a gold film was evaporated onto the sample *in situ* and the reflectance remeasured. The absolute reflectance is given by the ratio of these two measurements multiplied by the well-known reflectance of gold.[20]

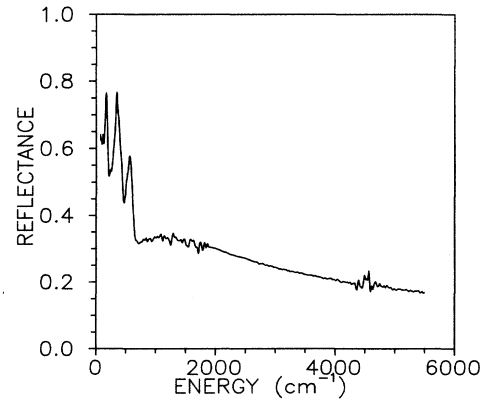

FIG. 3. Absolute reflectance of $LaTiO_3$ vs frequency at 300 K.

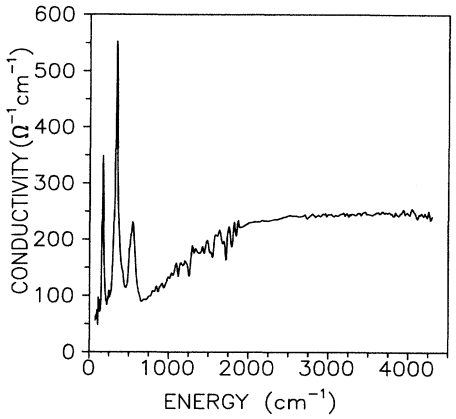

FIG. 4. Real optical conductivity vs frequency derived by Kramers-Kronig transformation of the reflectance.

Sample reflectance spectra are shown in Fig. 3. Note the three prominent groups of phonons near 170, 340, and 520 cm^{-1} and the nonzero reflectance above the highest optical-phonon frequency near 600 cm^{-1}.

Kramers-Kronig analysis was used to obtain $\sigma(\omega)$ and the results are shown in Fig. 4. A low-frequency Drude extrapolation was used which was consistent with both the measured dc resistivity ($\approx$24 mΩ cm) and the reflectance data. Different high-frequency extrapolations were used to estimate the uncertainty in the Kramers-Kronig analysis. The same results were obtained using either a constant reflectivity or the high-frequency reflectance of $SrTiO_3$ as measured by Cardona.[21] Note that no zero-frequency Drude absorption is resolved, although at low frequencies $\sigma(\omega)$ tends toward the dc value of $\approx 42\ \Omega^{-1}\,cm^{-1}$, as indicated in Fig. 5. The optical conductivity shows considerable structure: three groups of phonons near 170, 340, and 520 cm^{-1} and the onset of a broad absorption near 600 cm^{-1}.

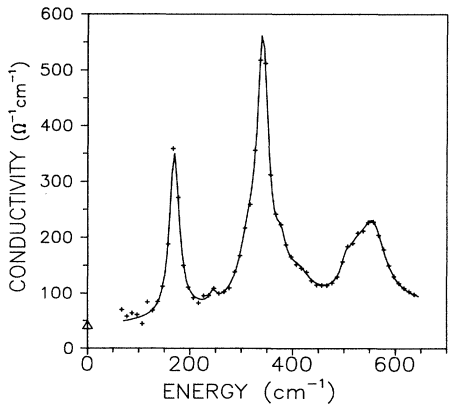

FIG. 5. Expanded view of the low-frequency optical conductivity of $LaTiO_3$ showing phonon structure. —— is the least-squares fit of Eq. (1) to the experimental data (+++). The fitting parameters appear in Table I. The dc conductivity is indicated by Δ in the diagram.

IV. DISCUSSION

A. Phonons

One can explain the phonon features in $\sigma(\omega)$ by using the factor group analysis of Couzi and Huong,[22] who considered both the ideal cubic perovskite structure and orthorhombically distorted $GdFeO_3$, which has the same structure as $LaTiO_3$. The cubic perovskites have 12 optical-phonon branches, three triply degenerate infrared-active F_{1u} branches, and one infrared-inactive F_{2u} branch. Orthorhombically distorted $LaTiO_3$ with four formula units per unit cell has 57 optical modes. According to Couzi and Huong, the orthorhombic distortion causes a 12-fold splitting of each F_{1u} mode, five of which are infrared active. There is also a 12-fold splitting of the F_{2u} mode; however, only four of these become ir active. Finally the orthorhombic distortion produces nine new modes $(3A_u+2B_{1u}+2B_{2u}+2B_{3u})$ for a maximum of 28 infrared active modes.

Figure 5 is an expanded view of the low-frequency $\sigma(\omega)$ of $LaTiO_3$. One can resolve a peak at 169 cm^{-1}, three peaks near 340 cm^{-1}, three peaks near 530 cm^{-1}, and shoulders at 245 and 411 cm^{-1}. A least-squares fit of of $\sigma(\omega)$ to the following formula (a set of nine Lorentzian oscillators plus a three-term polynomial background) converged to the parameters listed in Table I:

$$\sigma(\omega)=a+b\omega+c\omega^2+\frac{\omega}{60}\sum_{i=1}^{9}\frac{\omega\Gamma_i\omega_{pi}^2}{(\omega_{0i}^2-\omega^2)^2+\Gamma_i^2\omega^2} . \quad (1)$$

In Eq. (1), $\sigma(\omega)$ is in $\Omega^{-1}\,cm^{-1}$ while the phonon position (ω_{oi}), width (Γ_i), and strength (ω_{pi}) are in cm^{-1}. One interpretation of the spectrum is for the three strongest peaks to derive from the F_{1u} modes of the cubic lattice and the weak peaks near 245 and 411 cm^{-1} to derive from either the F_{2u} mode or the acoustic mode of the cubic lattice. This is the assignment suggested by Couzi and Huong for their infrared transmission measurements[22] performed on the rare-earth (R) orthochromites ($RCrO_3$). Broad absorption bands were observed near 200, 400, and 580 cm^{-1} in all the members of the series. A mode near 380 cm^{-1} becomes stronger in the heavier, more distorted members of the series and Couzi and Huong maintain that this mode is related to the F_{2u} mode of the cubic structure.

Very-low-frequency optical modes have been observed in $SrTiO_3$ and $BaTiO_3$. The F_{1u} modes have been observed[23] in cubic $SrTiO_3$ at 88, 176, and 544 cm^{-1} and in BaTiO at 34, 180, and 500 cm^{-1}. The possibility of a mode below 70 cm^{-1} that is not observed in the present measurements leads one to a second interpretation of the spectra. In this case the cluster of modes near 340 cm^{-1} derives instead from the F_{2u} mode of the cubic lattice and the shoulders near 220 and 420 cm^{-1} derive from acoustic modes in the cubic lattice. In either case it is likely that the modes near 170 and 520 cm^{-1} derive from the F_{1u} modes of the cubic lattice which correspond to vibrations where the La ion moves against the TiO_6 octahedra and an internal vibration of the TiO_6 octahedra, respectively.

Clearly, measurements on other rare-earth titanates would help with the mode assignments. The orthorhombic distortion increases in heavier members of the series. The mode deriving from the F_{2u} should increase its optical activity, and the fivefold splittings of the three main modes should become more pronounced allowing for a definite assignment.

TABLE I. Parameters of least-squares fit of Eq. (1) to the low-frequency optical conductivity of $LaTiO_3$. The polynomial background is $40+0.114\omega+9.47\times10^{-5}\omega^2$. All frequencies and dampings are in cm^{-1}.

i	ω_{0i}	Γ_i	ω_{pi}
1	169.4	23.3	636
2	245.3	15.5	136
3	314.9	48.7	542
4	341.8	26.4	829
5	377.3	26.4	300
6	410.7	59.7	374
7	503.7	22.4	190
8	522.9	51.4	427
9	556.9	57.8	654

B. Carrier absorption and the midinfrared band

The optical and transport properties are intimately related and should be explained self-consistently. Any model should be able to explain the midinfrared band in $\sigma(\omega)$ and the change from insulating to metallic behavior observed in resistivity.

It is instructive to compare the measured low frequency $\sigma(\omega)$ with the Drude model. The comparison shows that the electrons are somewhat localized. The contribution of free carriers to the optical conductivity is given by Eq. (2):

$$\sigma(\omega)=\frac{\sigma_{dc}\Gamma^2}{\omega^2+\Gamma^2} . \quad (2)$$

The scattering rate Γ is fixed by the dc conductivity σ_{dc} and the carrier density by the following relation:

$$\sigma_{dc}=\frac{ne^2}{m\Gamma} , \quad (3)$$

where n is the carrier concentration, e is the electron charge, and m is the band mass. Equation (2) is compared with the measured $\sigma(\omega)$ in Fig. 6 for three different carrier densities. A dc conductivity of 42 $\Omega^{-1}\,cm^{-1}$ was taken from the resistivity measurements (Fig. 2) and it was assumed that $m=10$, which is reasonable since it is believed that the metallic properties of $LaTiO_3$ are associated with electrons coming from Ti orbitals.[1] Note that assuming $n\gg10^{20}$ cm^{-3} yields the constant $\sigma(\omega)\approx\sigma_{dc}$ for frequencies below 200 cm^{-1}. Equation (2) only comes close to agreeing with the measured spectrum for concentrations greater than approximately 10^{20} cm^{-3}. What this means, however, is that the carrier mobility ($e/m\Gamma$) is less than or equal to 3 $cm^2/V\,s$. In addition to the

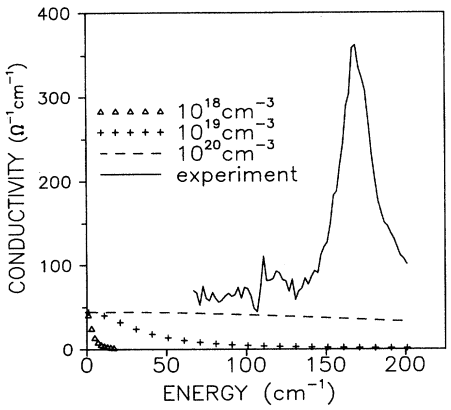

FIG. 6. Comparison of low-frequency optical conductivity with the Drude model [Eq. (2)]. The extrapolations assume a dc conductivity of 42 $\Omega^{-1}\,\mathrm{cm}^{-1}$ and an effective mass of 10. $\Gamma=3.57$, 35.7, and 357 cm^{-1} for carrier densities 10^{18}, 10^{19}, and 10^{20} cm^{-3} respectively. Carrier densities of 10^{21} and 10^{22} cm^{-3} would produce $\sigma(\omega)\approx\sigma_{dc}$ for frequencies below 200 cm^{-1}. The figure suggests a lower limit on the carrier concentration at approximately 10^{20} cm^{-3}.

midinfrared absorption band and the resistivity minimum, any model should account for the low carrier mobility in $LaTiO_3$.

In an overly simple narrow-band semiconductor model, the dc conductivity would be given by[24]

$$\sigma(T)=C\int_0^\infty \frac{x^{1/2}dx}{\exp[(x-\zeta)]+1}\ , \tag{4}$$

where C is a constant and $\zeta=E_g/2kT$. The midinfrared band of Fig. 4 could indicate a band gap (E_g) approximately equal to 550 cm^{-1}. This formula assumes acoustic-phonon scattering, and equal electron and hole band masses, and is compared to the measured resistivity data ($1/\sigma$) in Fig. 2. This model cannot reproduce the observed resistivity minimum, even if other scattering mechanisms are included. In addition, typical semiconductors usually have higher mobilities (e.g., the room-temperature electron mobilities of Si and GaP are 1500 and 110 $\mathrm{cm}^2/\mathrm{V\,s}$, respectively[25]).

Polarons have been considered in other oxides (e.g., TiO_2, $BaTiO_3$, and $SrTiO_3$) with equally low mobilities.[11] A small polaron model[26] has been tried and can reproduce the resistivity minimum assuming constant carrier density and a small activation energy (15 meV). The optical conductivity spectrum of small polarons has a broad peak at nonzero frequency which some workers have claimed to have observed in reduced TiO_2 near 0.8 eV.[13] Conceivably, the broad midinfrared absorption seen in Fig. 4 could also be a small polaron absorption band, but more work must be done to establish the correspondence. Specifically, the peak should scale with the dc conductivity which would require a measurement of the $\sigma(\omega)$ of various samples with different oxygen stoichiometries. Second, the band should exhibit the strong temperature dependence predicted by the theory.[27]

Note that in the sample studied, the broad resistivity minimum does not coincide with the magnetic transition. This is in contrast to previous measurements,[2] where both occurred at 125 K. Stoichiometric differences are obviously playing an important role, but one might conclude that the change from metallic to insulating behavior is not caused by antiferromagnetic ordering as had been previously suggested.[2] The work of Lichtenberg *et al.* suggests the resistivity minimum is characteristic only of oxidized material[6] and is not intrinsic to $LaTiO_3$. Rare-earth vacancies to which the rare-earth transition metal perovskites are susceptible[2] were not mentioned in this paper and more work should be done on the phase diagram of $LaTiO_x$ before concluding what is intrinsic to $LaTiO_3$. Temperature-induced metal-insulator transitions accompanied by small but abrupt changes in crystal structure have recently been observed in $PrNiO_3$ and $NdNiO_3$, which share the same orthorhombically distorted perovskite structure as $LaTiO_3$.[28] In $LaTiO_3$, no structural anomalies have been observed at temperatures near the resistivity minimum.[19]

V. CONCLUSIONS

Although a satisfactory theory that could explain the optical and transport properties self-consistently has not been found, the present measurements have established that the carriers in $LaTiO_3$ are somewhat localized. This is consistent with the magnetic ordering which occurs below 125 K.

Recently Torrance *et al.*[10] have shown that the model of Zaanen, Sawatsky, and Allen[29] (ZSA) can successfully explain the wide range of dc conductivities observed in simple and perovskite related metallic oxides. In this model, there are two relevant energies: Δ, the charge-transfer gap between filled oxygen orbitals and the lowest unoccupied metallic d state; and U', the energy separating the first unoccupied d state from the highest occupied d state. (U' is not always the Hubbard U.) Metallic behavior can result when either of the two gaps approaches zero. In their calculations, Torrance *et al.* show that for $LaTiO_3$ Δ is large, but U' lies right on the boundary separating insulating high-U materials from metallic low-U materials; in the ZSA scheme, $LaTiO_3$ is on the verge of being a low-U metal. The optical and transport measurements reported above support this view of $LaTiO_3$ as a barely metallic material.

ACKNOWLEDGMENTS

We thank David Singh for performing the band-structure calculation, and we appreciate the assistance of Jim Garrett, Frank Gibbs, Wen He Gong, Maureen Reedyk, and C. V. Stager. This work was supported at McMaster by the Natural Science and Engineering Research Council of Canada (NSERC), including infrastructure support for the Institute for Materials Research.

[1]J. E. Greedan, J. Less-Common Met. **111**, 335 (1985).
[2]David A. MacLean and J. E. Greedan, Inorg. Chem. **20**, 1025 (1980).
[3]P. Ganguly, Om. Parkash, and C. N. R. Rao, Phys. Status Solidi A **36**, 669 (1976).
[4]G. V. Bazuev and G. P. Shveikin, Inorg. Mater. **14**, 201 (1978).
[5]J. P. Goral and J. E. Greedan, J. Magn. Magn. Mater. **37**, 315 (1983).
[6]F. Lichtenberg, D. Widmer, J. G. Bednorz, T. Williams, and A. Reller, Z. Phys. B **82**, 211 (1991).
[7]Y. Maeno, S. Awaji, H. Matusmoto, and T. Fujita, Physica B **165-166**, 1185 (1990).
[8]David Singh (private communication).
[9]N. F. Mott, *Metal-Insulator Transitions* (Taylor & Francis, London, 1974), p. 31.
[10]J. B. Torrance, P. Lacorre, Chinnarong Asavaroengchai, and R. M. Metzger, J. Solid State Chem. **90**, 168 (1991).
[11]J. M. Honig, IBM J. Res. Dev. **14**, 232 (1970).
[12]D. Adler and J. Feinleib, Phys. Rev. B **2**, 3112 (1970).
[13]V. N. Bogomolov, E. K. Kudinov, D. N. Mirlin, and Yu. A. Firsov, Fiz. Tverd. Tela (Leningrad) **9**, 2077 (1967) [Sov. Phys. Solid State **9**, 1630 (1968)].
[14]E. K. Kudinov, D. N. Mirlin, and Yu. A. Firsov, Fiz. Tverd. Tela (Leningrad) **11**, 2789 (1969) [Sov. Phys. Solid State **11**, 2257 (1970)].
[15]A. S. Barker, Jr., H. W. Verleur, and H. J. Guggenheim, Phys. Rev. Lett. **17**, 1286 (1966).
[16]H. W. Verleur, A. S. Barker, Jr., and C. N. Berglund, Phys. Rev. **172**, 788 (1968).
[17]S. Uchida, T. Ido, H. Takagi, T. Arima, Y. Tokura, and S. Tajima, Phys. Rev. B **43**, 7942 (1991).
[18]S. L. Cooper, G. A. Thomas, J. Orenstein, D. H. Rapkine, A. J. Millis, S.-W. Cheong, and A. S. Cooper, Phys. Rev. B **41**, 11 605 (1990).
[19]Manfred Eitel and J. E. Greedan, J. Less-Common Met. **116**, 95 (1986).
[20]*Handbook of Optical Constants of Solids,* edited by Edward D. Palik (Academic, New York, 1985).
[21]M. A. Cardona, Phys. Rev. **140**, A651, 1965.
[22]M. Couzi and P. Vam Huong, J. Chim. Phys. **69**, 1339 (1972).
[23]A. S. Barker, Jr., Phys. Rev. **145**, 391 (1966).
[24]R. A. Smith, *Semiconductors* (Cambridge University Press, Cambridge, 1978), Chap. 4.8.
[25]S. M. Sze, *Physics of Semiconductor Devices* (Wiley, New York, 1981), p. 849.
[26]I. G. Austin and N. F. Mott, Adv. Phys. **18**, 41 (1969).
[27]H. G. Reik and D. Heese, J. Phys. Chem. Solids **28**, 581 (1967).
[28]P. Lacorre, J. B. Torrance, J. Pannetier, A. I. Nazzal, P. W. Wang, and T. C. Huang, J. Solid State Chem. **91**, 225 (1991).
[29]J. Zaanen, G. A. Sawatsky, and J. W. Allen, Phys. Rev. Lett. **55**, 418 (1985).